



STRUCTURAL  
BIOLOGY

**Volume 76 (2020)**

**Supporting information for article:**

**Crystal structures of peanut lectin in the presence of synthetic  $\beta$ -N- and  $\beta$ -S-galactosides disclose evidence for the recognition of different glycomimetic ligands**

**Alejandro J. Cagnoni, Emiliano D. Primo, Sebastián Klinke, María E. Cano, Walter Giordano, Karina V. Mariño, José Kovensky, Fernando A. Goldbaum, María Laura Uhrig and Lisandro H. Otero**

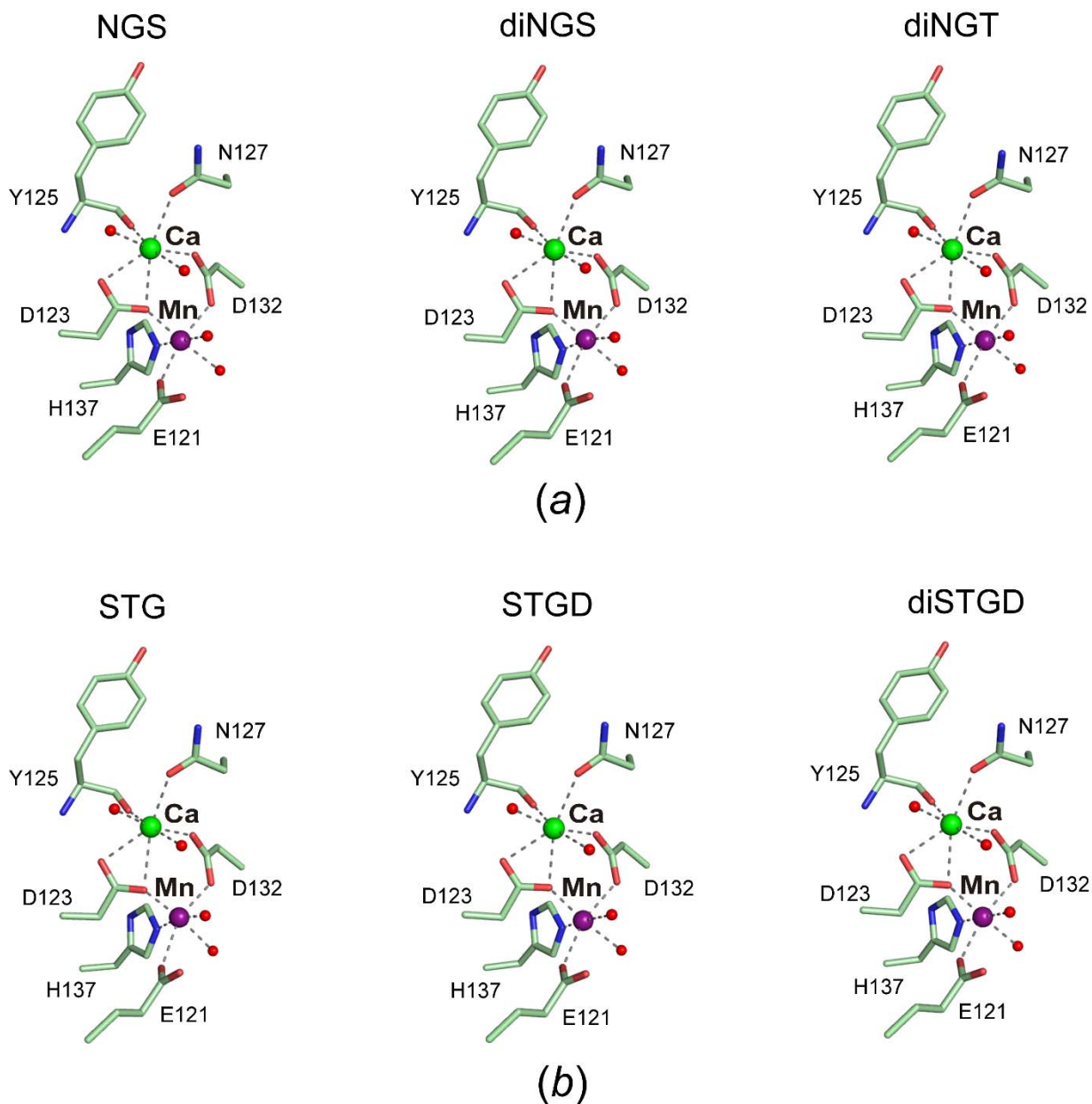


**Figure S1** Metal binding sites near the sugar-binding pocket of PNA in complex with the different synthetic glycoclusters. (a) N-linked glycoclusters NGS, diNGS, and diNGT. (b) S-linked glycoclusters STG, STGD, and diSTGD. Mn<sup>2+</sup> and Ca<sup>2+</sup> ions are indicated. The residues involved in the metal interactions are labeled and colored according to Fig. 4. Water molecules are shown as red spheres.

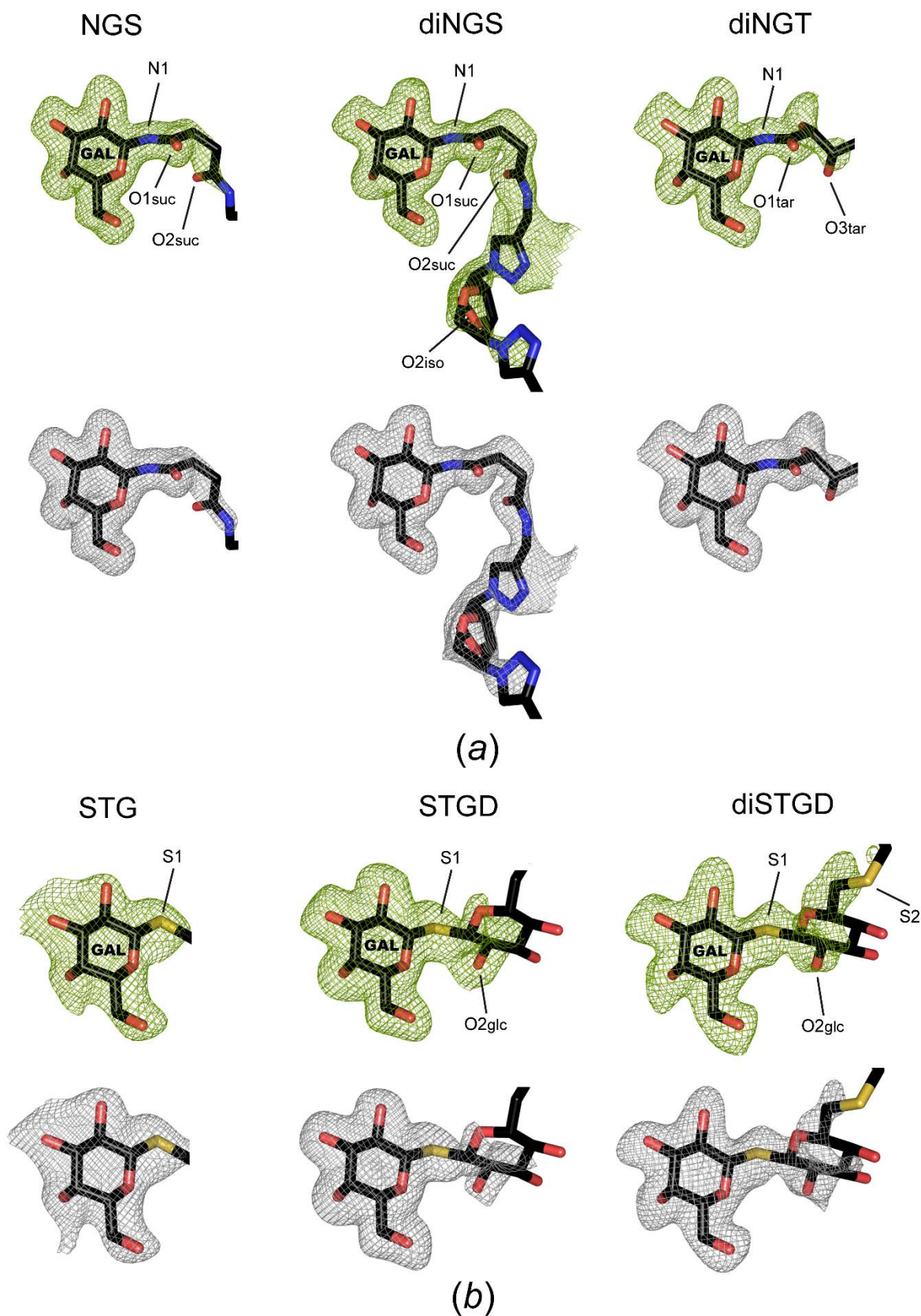


**Figure S2** Final *mFo*-*DFc* omit and *mFo*-*DFc* polder omit maps around the bound synthetic glycoclusters. (a) N-linked glycoclusters NGS, diNGS, and diNGT. (b) S-linked glycoclusters STG, STGD, and diSTGD. Labels,

orientations and representations are similar as in Figure 3. Only ligand portions defined by the electron density maps are shown. Omit maps (green mesh) and polder omit maps (gray mesh) are contoured at  $2.5 \sigma$  evidencing the presence of the ligands. Omit maps were generated by removing the ligands from the models followed by five cycles of refinement in PHENIX (Adams *et al.*, 2010). The polder maps excluding the bulk solvent around the omitted region were generated using the “Polder Maps” tool (Liebschner *et al.*, 2017) in PHENIX.

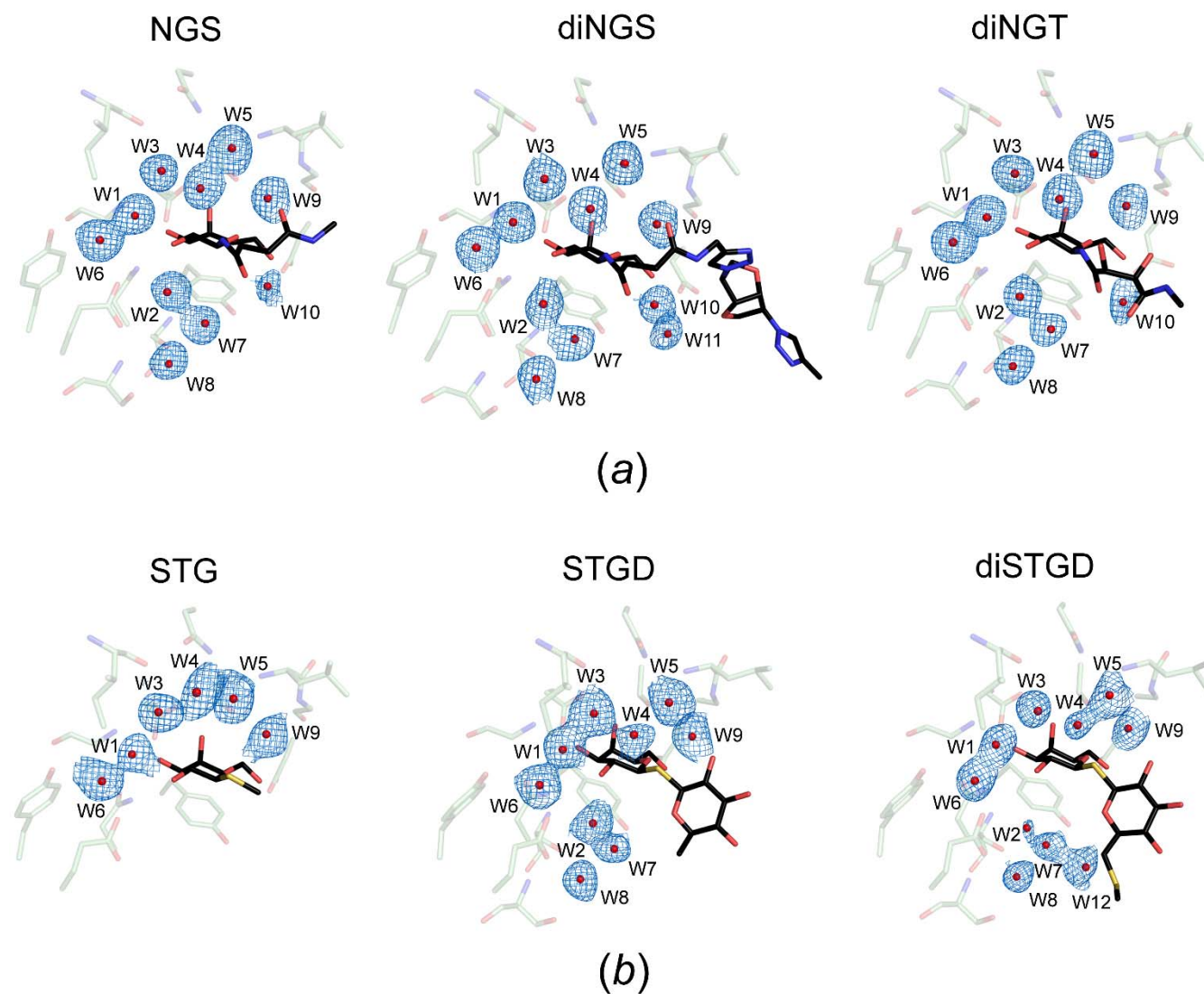


**Figure S3** Final  $2mF_o - DF_c$  electron density maps around the bound water molecules at the sugar-binding pocket of PNA in complex with the different synthetic glycoclusters. (a) N-linked glycoclusters NGS, diNGS, and diNGT. (b) S-linked glycoclusters STG, STGD, and diSTGD. Similar views with respect to Fig. 4 are shown in all cases. The maps (blue mesh) are contoured at  $1.0 \sigma$ . Water molecules in the active site are shown as red spheres. The ligands and the most relevant residues involved in the interactions are colored according to Fig. 4. Only ligand portions defined by the electron density maps are shown. The maps were generated in PHENIX (Adams *et al.*, 2010).

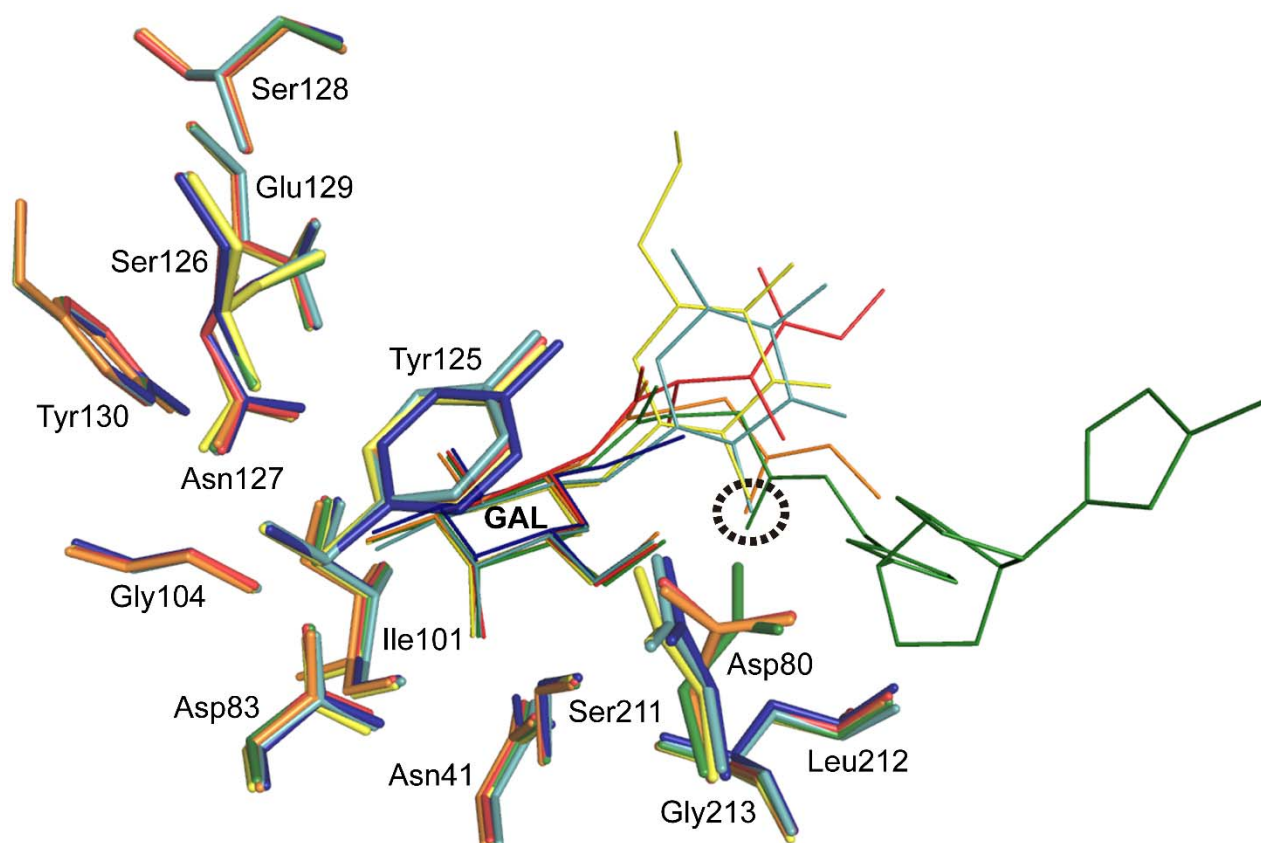
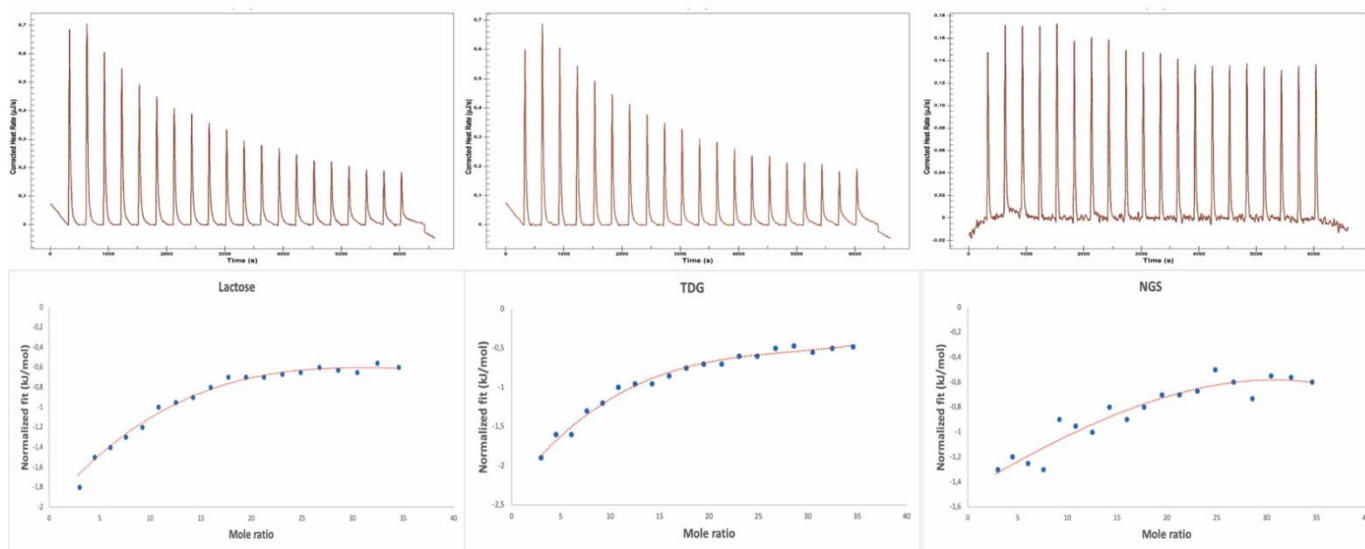


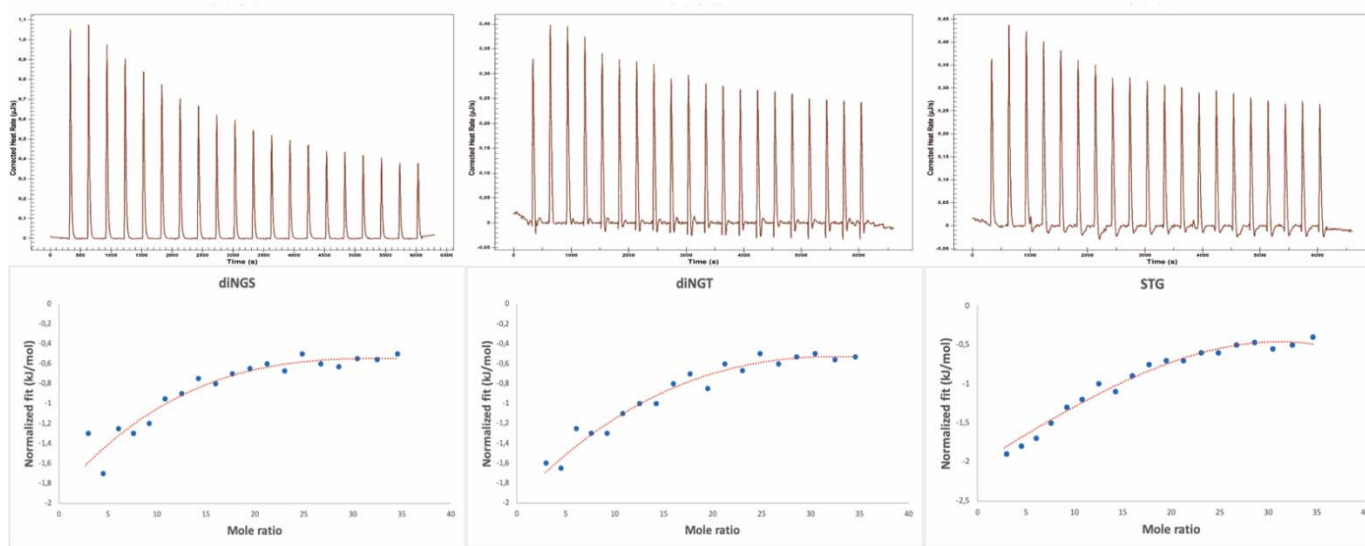
**Figure S4** Ligand binding structural comparison amongst the different PNA-synthetic glycocluster complexes. The protein-ligand complexes are colored as follows: PNA-NGS, orange; PNA-diNGS, green; PNA-diNGT, red; PNA-STG, blue; PNA-STGD, cyan; and PNA-diSTGD, yellow. The most relevant residues involved in the interactions are depicted as sticks. The ligands are shown as lines and colored according to the complex. Only the ligand portions defined by the electron density maps are shown. With a dashed black circle, the analogous positions between the atoms  $O_{2_{glc}}$  from the thioglycoclusters (STGD and diSTGD) and  $O_{2_{suc}}$  from the succinimidyl chains (NGS and diNGS) are highlighted. The galactose moiety is labeled for clarity.



(a)

(b)

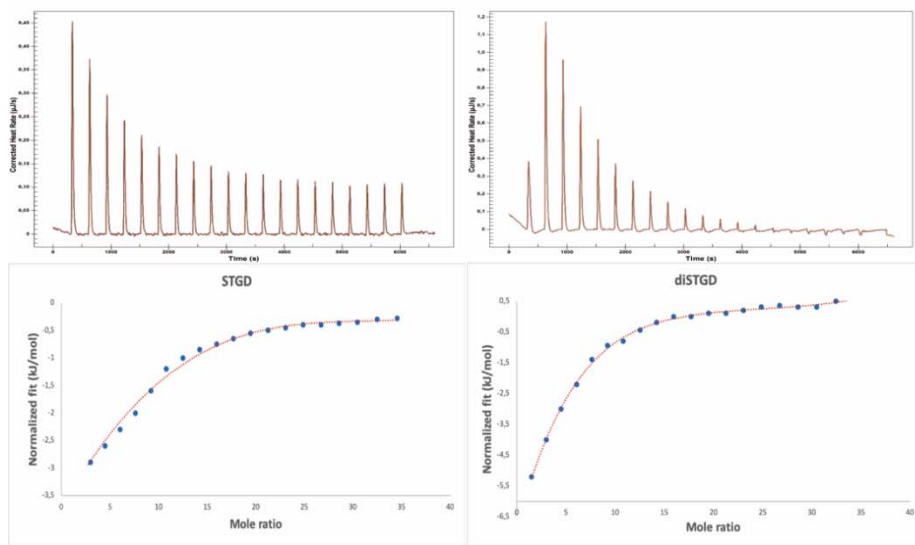
(c)



(d)

(e)

(f)



(g)

(h)

**Figure S5** Interaction analysis of the synthetic glycoclusters with PNA by ITC. **Thermograms and** integrated heats of interaction between PNA and (a) lactose, (b) TDG, (c) NGS, (d) diNGS, (e) diNGT, (f) STG, (g) STGD, and (h) diSTGD at 298 K. The independent model was implemented using the NanoAnalyze software to obtain the fitting curve for the experimental data.